Direct observation and temperature control of the surface Dirac gap in a topological crystalline insulator

B.M. Wojek[1], M.H. Berntsen[1], V. Jonsson[1,2], A. Szczerbakow[3], P. Dziawa[3], B.J. Kowalski[3], T. Story[3] & O. Tjernberg[1,2]

Since the advent of topological insulators hosting Dirac surface states, efforts have been made to gap these states in a controllable way. A new route to accomplish this was opened up by the discovery of topological crystalline insulators where the topological states are protected by crystal symmetries and thus prone to gap formation by structural changes of the lattice. Here we show a temperature-driven gap opening in Dirac surface states within the topological crystalline insulator phase in (Pb,Sn)Se. By using angle-resolved photoelectron spectroscopy, the gap formation and mass acquisition is studied as a function of composition and temperature. The resulting observations lead to the addition of a temperature- and composition-dependent boundary between massless and massive Dirac states in the topological phase diagram for (Pb,Sn)Se (001). Overall, our results experimentally establish the possibility to tune between massless and massive topological states on the surface of a topological system.

[1] KTH Royal Institute of Technology, ICT MNF Materials Physics, Electrum 229, 164 40 Kista, Sweden. [2] Center for Quantum Materials, Nordic Institute for Theoretical Physics (NORDITA), Roslagstullsbacken 23, 106 91 Stockholm, Sweden. [3] Institute of Physics, Polish Academy of Sciences, Aleja Lotników 32/46, 02-668 Warsaw, Poland. Correspondence and requests for materials should be addressed to O.T. (email: oscar@kth.se).

The study of topological properties of materials and corresponding phase transitions has received tremendous interest in the condensed-matter community in recent years[1,2]. A particularly interesting class of materials are three-dimensional topological crystalline insulators (TCIs)[3,4] where degeneracies in the surface electronic band structures are protected by point-group symmetries of the crystals. The first material systems to realize this state were found within the class of IV–VI narrow-gap semiconductors: SnTe[5,6], (Pb,Sn)Te[7,8] and (Pb,Sn)Se[9,10]. These materials, crystallizing in the rock-salt structure, host a set of four Dirac points on specific surfaces and a great advantage in particular of the solid solutions is the tunability of the bulk band gap—and hence their topological properties—by several independent parameters[11], such as composition[8,12], temperature[9,10,12], pressure[13] or strain[14]. Moreover, since the surface Dirac points are protected by crystalline symmetries, it has been predicted that selectively breaking these symmetries can lift the surface-state degeneracies and the carriers acquire masses[5,15]. Indeed, signatures of such massive surface Dirac fermions have been observed recently in Landau-level-spectroscopy experiments on (001) surfaces of (Pb,Sn)Se crystals[16] and a surface distortion has been identified to be at the heart of the phenomenon[17] (Fig. 1). However, since these scanning tunnelling microscopy/spectroscopy (STM/STS) studies only provide low-temperature data, the evolution of the surface-state mass/gap with temperature remains elusive. It is particularly interesting to ask whether the four (ungapped) Dirac points ever exist simultaneously on the (001) surface of (Pb,Sn)Se crystals in the TCI state, whether the partially gapped surface states can be observed directly by k-resolved methods, and whether one can switch between the massive and massless states by varying extrinsic parameters.

In this study, we address these open questions using high-resolution angle-resolved photoelectron spectroscopy (ARPES) measurements on (Pb,Sn)Se mixed crystals. Consistent with the previous STM/STS studies we directly observe robust gapped Dirac states on the (001) surface at low temperature. Most importantly, however, the evolution of the gap/mass is tracked by composition- and temperature-dependent experiments and a transition to entirely massless surface Dirac states is witnessed. We suggest that the surface distortion detected by STM vanishes at sufficiently high temperatures, thus leading to the possibility of tuning the surface states employing structural changes. Subsequently, this is summarized in a revised topological phase diagram for (Pb,Sn)Se (001).

Results

While studying the detailed nature of the bulk band inversion in (Pb,Sn)Se by high-resolution ARPES[12], low-temperature data of certain samples with comparably high SnSe content were found to contain a peculiar distribution of spectral weight around the Dirac points. An example of such spectra (not included in ref. 12) is depicted in Fig. 2a. The characteristic band structure of the hybridized parent surface Dirac cones schematically shown in Fig. 1 is clearly observed close to the $\overline{X}$ point of the (001) surface Brillouin zone. However, also a distinct gap opening $\Delta_{\overline{\Lambda_{\overline{X}}}}$ at the Dirac nodes $\overline{\Lambda_{\overline{X}}}$ on the $\overline{\Gamma}$-$\overline{X}$ line is revealed. Following this initial finding and reports of similar observations using STM/STS techniques[16], the gap formation has been studied systematically across the available temperature and composition ranges.

Our analysis (see Methods section) shows that most of the low-temperature spectra are gapped. Yet, at higher temperatures the Dirac nodes are—within the resolution of the experiment—overall intact. Figure 2b,c summarizes the ascertained gap sizes for the samples investigated during this study. While one has to
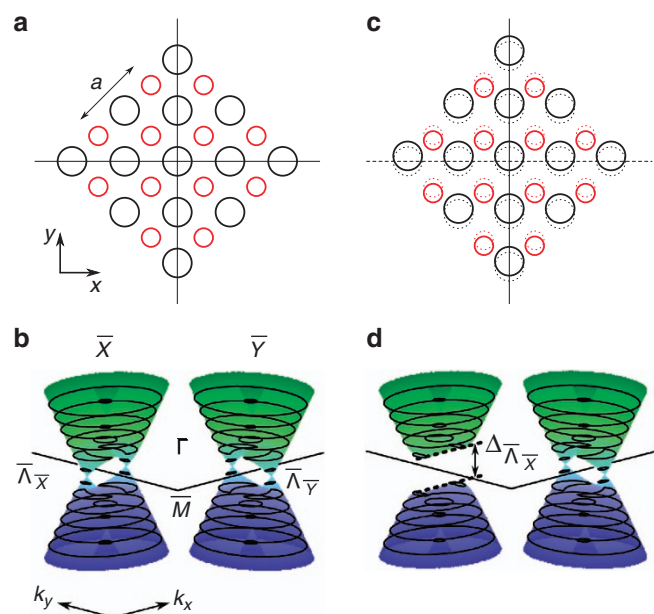

Figure 1 | The (001) surface and TCI surface band structure of (Pb,Sn)Se. (**a**) Sketch of the undistorted (001) surface with bulk lattice constant a. The black and red circles represent the cations and anions, respectively. The mirror lines of the surface are indicated by solid lines; (**b**) Sketch of the surface band structure corresponding to **a**. The particle-hole-symmetric band structure consists of the well-known hybridized Dirac cones, featuring a Lifshitz transition indicated by the constant-energy contours. The given labels denote the high-symmetry points of the surface Brillouin zone ($\overline{\Gamma}$, $\overline{M}$, $\overline{X}$, $\overline{Y}$) and the positions of the Dirac points ($\overline{\Lambda_{\overline{X}}}$, $\overline{\Lambda_{\overline{Y}}}$); (**c**) Sketch of a distorted (001) surface (solid circles) originating from the surface shown in **a** (dotted circles) by shifting the cation and anion sublattices with respect to each other along one of the mirror lines as suggested by STM measurements[17]. The dashed line indicates the breaking of the second mirror symmetry by this distortion; (**d**) Sketch of the surface band structure corresponding to **c**. The broken mirror symmetry induces a gap $\Delta_{\overline{\Lambda_{\overline{X}}}}$ in one pair of the surface states. In this work, x and y (and k_x and k_y, correspondingly) are defined in the surface as shown. These coordinates are rotated by 45° about z with respect to the conventionally used bulk coordinates.

note that the values of $\Delta_{\overline{\Lambda_{\overline{X}}}}$ vary by about 3–4 meV for nominally similar sample compositions, nevertheless, a general trend to larger values for higher SnSe contents and lower temperatures is apparent.

Having directly established the low-temperature mass acquisition of the Dirac fermions at $\overline{\Lambda_{\overline{X}}}$ it remains to be investigated whether the Dirac points at $\overline{\Lambda_{\overline{Y}}}$ do exist also on the distorted surface as suggested by the STM/STS studies[16,17]. Unlike STM/STS which is a local-probe technique, ARPES averages over a lateral sample region with a diameter of several tens of micrometres. Hence, a priori the observation of both massive surface states at $\overline{\Lambda_{\overline{X}}}$ and massless states at $\overline{\Lambda_{\overline{Y}}}$ requires a long-range textured surface. If rather a multidomain structure is formed with distortions along x and y, respectively for different domains, then, a superposition of gapped and gapless states is expected to be seen. A further complication arises from the low photon energy and the experimental geometry of the ARPES set-up which necessitate the samples under study to be rotated by $\pm 90°$ to enable the collection of electrons originating from $\overline{Y}$. Since most likely laterally slightly different parts of the surface are probed before and after such a manipulation, the long-range-texture precondition is further intensified. Our experiments show that this requirement is not always met (and hence, overall
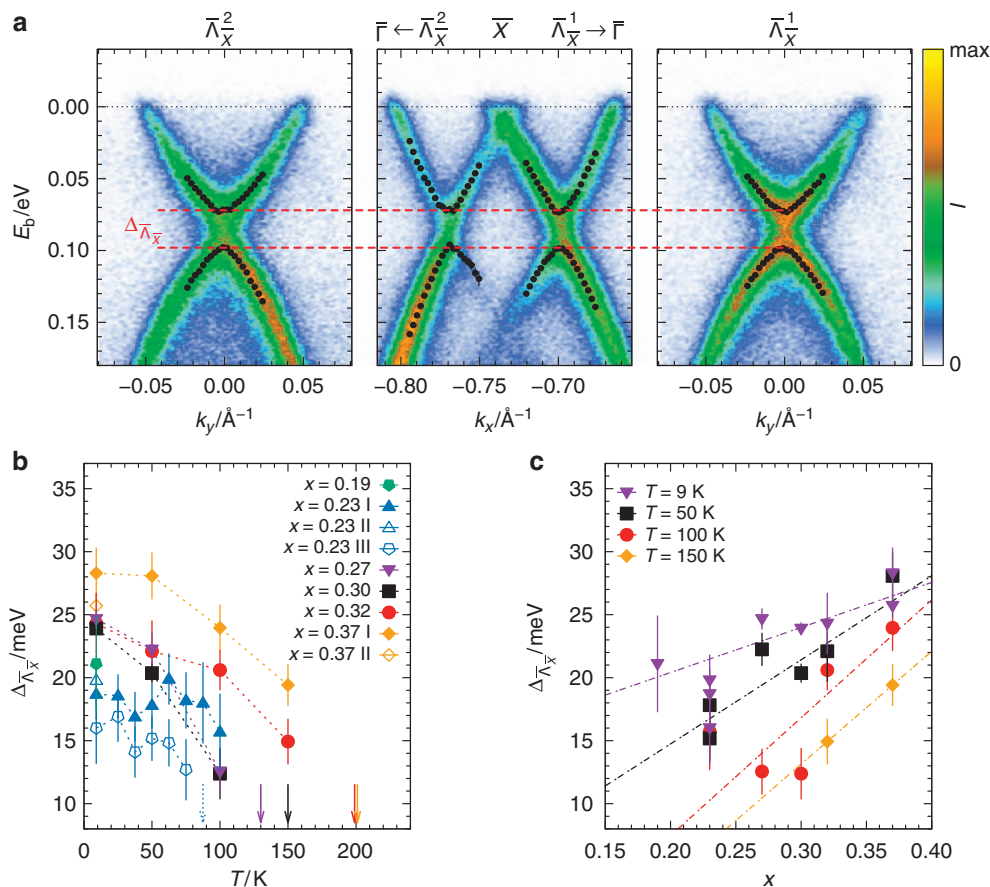
Figure 2 | Surface-state Dirac gap in (Pb,Sn)Se (001). (a) ARPES spectra showing the surface-state dispersion of $Pb_{0.63}Sn_{0.37}Se$ in the vicinity of $\overline{X}$ at $T = 9$ K. The reciprocal-space cuts are taken parallel to the borders of the surface Brillouin zone through the Dirac points at $\overline{\Lambda_{\overline{X}}}$ as labelled. The photoelectron intensity is encoded in a linear colour scale for each plot. The black circles represent the obtained peak positions from a two-Voigtian fit to the energy distribution curves. Vertical error bars correspond to the statistical uncertainties from the fit. A gap $\Delta_{\overline{\Lambda_{\overline{X}}}}$ of about 25 meV is observed consistently across the spectra; **(b)** Surface-state gap $\Delta_{\overline{\Lambda_{\overline{X}}}}$ as a function of temperature for various cleaved (001) surfaces of $Pb_{1-x}Sn_xSe$. Only gap values, which can be reliably determined by our analysis are shown. At higher temperatures $\Delta_{\overline{\Lambda_{\overline{X}}}}$ vanishes within the resolution of our experiment. The vertical arrows coloured equivalently to the data series indicate the lowest temperatures for which the Dirac points have been found intact within the experimental resolution. The dotted arrow corresponds to the series $x = 0.23$ III represented by open pentagons. Solid arrows belong to series marked by filled symbols. For data sets without corresponding arrows no gapless data in the TCI phase have been acquired. Since the density of data points in temperature varies substantially from one data set to another, the positions of the arrows cannot be simply interpreted as gap-closing temperatures; **(c)** $\Delta_{\overline{\Lambda_{\overline{X}}}}$ as a function of SnSe content x for selected temperatures. The dash-dotted lines indicate the rough trend in the observed gap size. The vertical error bars in **b,c** represent the statistical uncertainties from the energy-distribution-curve analysis scaled by a factor of 2 to take into account possible systematic shortcomings in the model used.

massive Dirac states are observed). Nevertheless, indeed we do find Dirac nodes, and thus massless states, at $\overline{\Lambda_{\overline{Y}}}$ coexisting with gapped states at $\overline{\Lambda_{\overline{X}}}$ at low temperatures. An example of the latter is shown in Fig. 3a through 3c. It illustrates the evolution of the (001) surface states of $Pb_{0.70}Sn_{0.30}Se$ across the different phases. Close to room temperature the sample is in a topologically trivial state characterized by the positive bulk gap at $\overline{X}$ (projection of the bulk high symmetry point L)[12]. On cooling to $T = 150$ K, the bulk bands invert and the sample enters the TCI phase with massless surface states. Lowering the temperature further leads to the gap formation at the positions of the former Dirac points $\overline{\Lambda_{\overline{X}}}$, while the degeneracies at $\overline{\Lambda_{\overline{Y}}}$ prevail, thus confirming the overall situation depicted in Fig. 1.

Discussion

To understand the full implications of this study, it is necessary and helpful to compare our results with the observations

made in STM/STS experiments before. Zeljkovic et al.[17] have demonstrated a low-temperature ($T = 4$ K) surface Dirac gap in (Pb,Sn)Se reaching a value of about 25 meV at a SnSe content of about 38% in the solid solution. With decreasing x the gap is reported to decrease and it supposedly vanishes at a critical composition of about 17%. At the same time, the observed lattice distortion at the surface appears to have roughly the same magnitude for all studied samples. To reconcile the diminishing surface gap, it has been argued that the penetration depth of the surface state into the bulk increases when the size of the bulk gap decreases and thus the weight of the surface state in the outermost atomic layer probed by STM/STS decreases continuously. So, is our observation of the (x, T)-dependent gap merely the result of the varying surface-state penetration depth $\left(\propto \Delta_{\overline{X}}^{-1} \right)$? The answer to that question is found in Fig. 2b,c. At $T = 9$ K, $\Delta_{\overline{\Lambda_{\overline{X}}}}$ indeed decreases with decreasing x, but in total only by a few millielectronvolts from $x = 0.37$ to $x = 0.19$. A similar behaviour is found at $x = 0.23$: On increasing the temperature from 9 K to

100 K (spanning essentially the entire band-inverted region) the observed gap is reduced only minutely. Hence, $\Delta_{\overline{\Lambda}_{\overline{X}}}$ observed here is—if at all—only to a small extent influenced by the changing penetration depth of the surface states. Thus, possibly due to the increased probing depth of low-energy ARPES as compared with STM/STS (nanometres instead of ångströms), the gap can rather be regarded as a direct measure of the size of the lattice distortion at the surface[15]. This conclusion is seemingly at variance with the claims of ref. 17, yet, it should be noted that in the STM/STS work the reliably determined gap sizes span a region between about 15 meV and 30 meV, in full agreement with our data. The nonobservation of distinct features in the STS spectra due to the diminishing spectral weight in the top-most atomic layer does not imply an overall vanishing surface-state gap for samples close to the transition.

Altogether, our observations are summarized in Fig. 3d. On the basis of the distinction of the massive and massless surface states in the bulk-band-inverted region we are able to determine a transition line below which the lattice distortion at least in the (001) surface occurs (Fig. 3e). Given the finite resolution of our experiment (in terms of energy as well as temperature), it should be regarded as a lower limit and hence the indicated TCI phase with completely massless surface states might occupy a somewhat smaller, yet still finite, area in the (x, T) phase diagram. Since STM also provided evidence for a lattice distortion in the topologically trivial phase at low temperature[17], although inaccessible by our spectroscopic method, we suspect the

transition to occur at finite temperatures in this phase of the solid solutions as well.

The (Pb,Sn)Se mixed crystals with a SnSe content in the studied range are found to crystallize in the rock-salt structure without bulk structural phase transitions. Nevertheless, the occurrence of a surface distortion further corroborated by this study should not entirely catch us by surprise. SnSe itself features an orthorhombic crystal structure[18] and various closely related IV–VI solid solutions undergo ferroelectric phase transitions[19]. Also, in (Pb,Sn)Se the transverse-optical phonon mode at Γ softens as the temperature is lowered and the SnSe content is increased[20]. Occasionally, for $Pb_{0.59}Sn_{0.41}Se$ even bulk structural changes were reported and found to be suppressed only with increasing carrier densities[21], suggesting displacive transitions driven by electron–phonon coupling[22,23].

It is too early to conclude on the exact mechanism which leads to the observed surface structure. Specifically, given the small but still clearly detectable variations between different measured samples with comparable SnSe content, it appears that the local nature of this lattice distortion somewhat depends on the details of each surface. However, its overall tunability by independent parameters inferred from the (x, T) phase diagram (Fig. 3e) lays the foundation for achieving a controlled mass generation in the topological surface Dirac states. It will be interesting to see in the future how other TCI surfaces behave[24,25], both of single crystals and of thin films[26,27], where controlled tuning of the crystal structure, for example, by strain, promises to be a viable avenue to
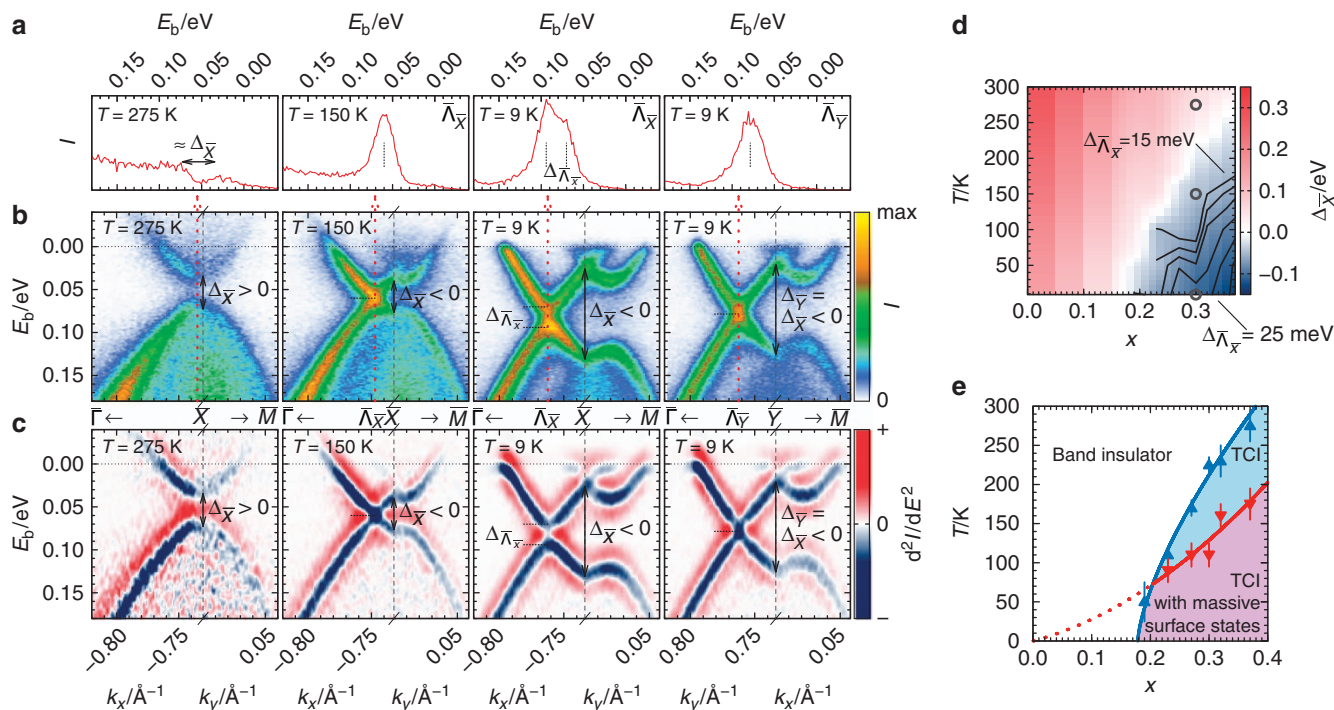

Figure 3 | Topological transitions in (Pb,Sn)Se (001). (a–c) ARPES data of $Pb_{0.70}Sn_{0.30}Se$ (001) at different temperatures in the vicinity of $\overline{X}/\overline{Y}$: (**b**) depicts the absolute photoelectron intensity along the high-symmetry lines of the surface Brillouin zone encoded in a linear colour scale; (**c**) The second derivative of the data in **b** with respect to the energy encoded in a linear colour scale; (**a**) EDCs along the red dotted lines in the spectra in **b**. The arrows in **b,c** indicate the fundamental bulk band gap $\Delta_{\overline{X}}$ inverting as a function of temperature. The black dotted lines mark the minimally separated EDC peaks and thus indicate the presence or absence of the surface Dirac gap $\Delta_{\overline{\Lambda}_{\overline{X}}}$; (**d**) Summary of the evolutions of the bulk gap ($\Delta_{\overline{X}}$, interpolated colour map, see also ref. 12) and the largest observed surface Dirac gap ($\Delta_{\overline{\Lambda}_{\overline{X}}}$, contour lines, spacing 2.5 meV) in $Pb_{1-x}Sn_xSe$ (001). The open grey circles indicate the (x, T) positions of the data shown in **a–c**; (**e**) Topological phase diagram for (Pb,Sn)Se (001) based on the observations of the spectral gaps shown in **d**. The symbols and corresponding error bars specify the temperature ranges in which the spectral changes shown throughout (**a–c**) occur. The red symbols estimate a lower temperature limit for the surface Dirac gap formation. The dotted line marks the proposed transition line for the occurrence of the surface distortion in the topologically trivial state. All lines are guides to the eye.

open gaps in topological surface states in addition to breaking symmetries by electric[28] or magnetic fields[15].

Eventually, it is worth noting that by specifically breaking both mirror symmetries as well as the rotational symmetries of the surface, all Dirac points are expected to be gapped in the material studied here[15]. If a domain structure is formed, then a topologically protected 1D conducting state percolating through the surface along the domain walls would be the result[5]. Such states can potentially be engineered in very thin films grown on specific vicinal surfaces or by employing TCIs naturally featuring suitable lattice distortions.

In summary, the evolution of the surface-state gap/mass in (Pb,Sn)Se (001) has been determined systematically by means of high-resolution ARPES. Our results are consistent with the proposed underlying surface distortion at low temperatures. The observation of only massless Dirac surface states at higher temperatures indicates a structural transition of the surface. While its detailed nature is yet to be investigated by systematic structural and/or vibrational studies, we have shown experimentally the possibility to tune between massive and gapless topological states using this very transition.

Methods

Crystal growth and characterization. The n-type (Pb,Sn)Se single crystals with typical doping levels of a few $10^{18}\,cm^{-3}$ studied in this work have been grown using the self-selecting vapour-growth method and characterized by X-ray diffraction and energy-dispersive X-ray spectroscopy[29,30]. High-resolution ARPES studies were carried out on samples cleaved in a (001) plane in ultrahigh vacuum at room temperature. Temperature-dependent measurements of solid solutions with SnSe/PbSe ratios between 0 and 0.6 were carried out at the BALTAZAR laser-ARPES facility using linearly polarized light with an excitation energy 10.5 eV and a THEMIS-1000 time-of-flight analyzer collecting the photoelectrons[31]. The overall crystal-momentum and energy resolution is better than $0.008\,\text{Å}^{-1}$ and about 5 meV, respectively.

Analysis of the photoelectron spectra. The decision whether the surface states in the TCI phase are massive/gapped is based on an analysis of the energy-distribution curves (EDCs) in the close vicinity of the Dirac nodes ($\bar{\Lambda}$). In a first step, the EDCs are modelled by sums of two Voigtian lines on a small strictly monotonic linear to cubic background. The resulting line widths are compared with a fit of a single Voigtian (on the same background) to the EDC at $\bar{\Lambda}$. In case the single line (full width at half maximum) at $\bar{\Lambda}$ is found to be broader by > 5 meV than the broadest two-line constituent, we call the states gapped and the two-line peak separation determines the gap size $\Delta_{\bar{\Lambda}}$. This criterion is based on the scattering of the determined line width at high temperatures and the energy resolution of the experiment, which are both on the order of 5 meV.

References

1. Hasan, M. Z. & Kane, C. L. Colloquium: topological insulators. *Rev. Mod. Phys.* **82,** 3045–3067 (2010).
2. Ando, Y. Topological insulator materials. *J. Phys. Soc. Jpn* **82,** 102001 (2013).
3. Fu, L. Topological crystalline insulators. *Phys. Rev. Lett.* **106,** 106802 (2011).
4. Ando, Y. & Fu, L. Topological crystalline insulators and topological superconductors: from concepts to materials. *Annu. Rev. Condens. Matter Phys.* **6,** 361–381 (2015).
5. Hsieh, T. H. *et al.* Topological crystalline insulators in the SnTe material class. *Nat. Commun.* **3,** 982 (2012).
6. Tanaka, Y. *et al.* Experimental realization of a topological crystalline insulator in SnTe. *Nat. Phys.* **8,** 800–803 (2012).
7. Xu, S.-Y. *et al.* Observation of a topological crystalline insulator phase and topological phase transition in $Pb_{1-x}Sn_xTe$. *Nat. Commun.* **3,** 1192 (2012).
8. Tanaka, Y. *et al.* Tunability of the k-space location of the Dirac cones in the topological crystalline insulator $Pb_{1-x}Sn_xTe$. *Phys. Rev. B* **87,** 155105 (2013).
9. Dziawa, P. *et al.* Topological crystalline insulator states in $Pb_{1-x}Sn_xSe$. *Nat. Mater.* **11,** 1023–1027 (2012).
10. Wojek, B. M. *et al.* Spin-polarized (001) surface states of the topological crystalline insulator $Pb_{0.73}Sn_{0.27}Se$. *Phys. Rev. B* **87,** 115106 (2013).
11. Nimtz, G. & Schlicht, B. in *Springer Tracts in Modern Physics,* Vol. 98 (ed. Hohler, G.) Ch. 1 (Springer-Verlag, 1983).
12. Wojek, B. M. *et al.* Band inversion and the topological phase transition in (Pb,Sn)Se. *Phys. Rev. B* **90,** 161202 (2014).
13. Barone, P. *et al.* Pressure-induced topological phase transitions in rocksalt chalcogenides. *Phys. Rev. B* **88,** 045207 (2013).
14. Barone, P., Di Sante, D. & Picozzi, S. Strain engineering of topological properties in lead-salt semiconductors,. *Phys. Status Solidi RRL* **7,** 1102–1106 (2013).
15. Serbyn, M. & Fu, L. Symmetry breaking and Landau quantization in topological crystalline insulators. *Phys. Rev. B* **90,** 035402 (2014).
16. Okada, Y. *et al.* Observation of Dirac node formation and mass acquisition in a topological crystalline insulator. *Science* **341,** 1496–1499 (2013).
17. Zeljkovic, I. *et al.* Dirac mass generation from crystal symmetry breaking on the surfaces of topological crystalline insulators. *Nat. Mater.* **14,** 318–324 (2015).
18. Wiedemeier, H. & von Schnering, H. G. Refinement of the structures of GeS, GeSe, SnS and SnSe. *Z. Kristallogr.* **148,** 295–303 (1978).
19. Lebedev, A. I. & Sluchinskaya, I. A. Ferroelectric phase transitions in IV–VI semiconductors associated with off-center ions. *Ferroelectrics* **157,** 275–280 (1994).
20. Vodop'yanov, L. K., Kucherenko, I. V., Shotov, A. P. & Scherm, R. Zero-gap state and phonon spectrum of the system of narrow-band compounds $Pb_{1-x}Sn_xSe$. *JETP Lett.* **27,** 92–95 (1978).
21. Volkov, B. A., Kucherenko, I. V., Moiseenko, V. N. & Shotov, A. P. Structural phase transition in the $Pb_{1-x}Sn_xSe$ system under the influence of temperature and hydrostatic pressure. *JETP Lett.* **27,** 371–374 (1978).
22. Volkov, B. A. & Pankratov, O. A. Crystal structures and symmetry of the electron spectrum of IV–VI semiconductors. *J. Exp. Theor. Phys.* **48,** 687–696 (1978).
23. Konsin, P. Microscopic theory of ferroelectric phase transitions in $A^{IV}B^{VI}$-type semiconductors. *Ferroelectrics* **45,** 45–50 (1982).
24. Safaei, S., Kacman, P. & Buczko, R. Topological crystalline insulator (Pb,Sn)Te: Surface states and their spin polarization. *Phys. Rev. B* **88,** 045305 (2013).
25. Liu, J., Duan, W. & Fu, L. Two types of surface states in topological crystalline insulators. *Phys. Rev. B* **88,** 241303 (2013).
26. Yan, C. *et al.* Experimental observation of Dirac-like surface states and topological phase transition in $Pb_{1-x}Sn_xTe(111)$ films. *Phys. Rev. Lett.* **112,** 186801 (2014).
27. Polley, C. M. *et al.* Observation of topological crystalline insulator surface states on (111)-oriented $Pb_{1-x}Sn_xSe$ films. *Phys. Rev. B* **89,** 075317 (2014).
28. Liu, J. *et al.* Spin-filtered edge states with an electrically tunable gap in a two-dimensional topological crystalline insulator. *Nat. Mater.* **13,** 178–183 (2014).
29. Szczerbakow, A. & Berger, H. Investigation of the composition of vapour-grown $Pb_{1-x}Sn_xSe$ crystals ($x \leq 0.4$) by means of lattice parameter measurements. *J. Cryst. Growth* **139,** 172–178 (1994).
30. Szczerbakow, A. & Durose, K. Self-selecting vapour growth of bulk crystals—Principles and applicability. *Prog. Cryst. Growth Charact. Mater.* **51,** 81–108 (2005).
31. Berntsen, M. H., Götberg, O. & Tjernberg, O. An experimental setup for high resolution 10.5 eV laser-based angle-resolved photoelectron spectroscopy using a time-of-flight electron analyzer. *Rev. Sci. Instrum.* **82,** 095113 (2011).

Acknowledgements

Author contributions

B.M.W. and O.T. planned the study. A.S. and P.D. synthesized and characterized the studied materials. B.M.W., M.H.B. and V.J. performed the photoemission experiments. B.M.W. analysed the data and wrote the manuscript with input from all authors. All authors contributed to the interpretation of the data.

Additional information

Competing financial interests: The authors declare no competing financial interests.

Reprints and permission information is available online at http://npg.nature.com/reprintsandpermissions/

How to cite this article: Wojek, B. M. *et al.* Direct observation and temperature control of the surface Dirac gap in a topological crystalline insulator. *Nat. Commun.* 6:8463 doi: 10.1038/ncomms9463 (2015).